Multiphysics Simulation of Metal Solidification Processes with Abaqus

Seid Koric, Brian G. Thomas, and Lance C. Hibbeler

National Center for Supercomputing Applications-NCSA &
Mechanical Science and Engineering Department
University of Illinois at Urbana-Champaign
1205 W. Clark Street
Urbana, IL 61801
USA

A coupled thermo-mechanical model of solidifying shell (Koric, 2006, 2011), (Hibbeler, 2009) in Abaqus/Standard is combined with turbulent fluid flow in the liquid pool and thermal distortion of the mold to create an accurate multiphysics model of steel continuous casting. The new model is applied to calculate temperature stress and deformation in a commercial beam blank caster with complex geometry. Results from the complete system compare favorably with plant measurements of shell thickness.

Keywords: Material Processing, Solidification, Steel Continuous Casting, Thermal Stress Tubulent Fluid Flow, Enhanced Latent Heat, Multiphysics, Finite Elements, Abaqus

1. Introduction and Previous Work

Many manufacturing and fabrication processes such as foundry shape casting, continuous casting and welding have common solidification phenomena. One of the most important and complex of these is continuous casting, which produces 90% of steel today. Even though the process is constantly improving, there is still a significant need to minimize defects and to maximize quality and efficiency.

The difficulty of plant experiments under harsh operating conditions makes computational modeling an important tool in the design and optimization of these processes. Increased computing power and better numerical methods have enabled researchers to develop better models of many different aspects of these processes. Coupling together the different models of heat transfer, solidification distortion, stress generation in newly formed solid and turbulent fluid flow to make accurate predictions of the entire real processes remains a challenge.

At the same time the increasing power of computers and development of numerical methods in the last 30 years has helped researchers to better understand the governing principles of various material processing operations. The continuous casting process is not exception, and it has been subjected to more numerical models than any other process. However, it is a challenging task too,

and there is large number of computational difficulties encountered with numerical modeling of thermo-mechanical behavior of the shell in continuous casting.
In 1963, Weiner and Boley (Weiner, 1963) derived a semi-analytical solution for the thermal stresses arising during the solidification of a semi infinite plate. Although that work oversimplifies the complex physical phenomena of solidification, it has become a useful benchmark problem for the verification of numerical models (Zhu, 1993, Li, 2004, Koric, 2006). The constitutive models used in previous work to investigate thermal stresses during continuous casting first adopted simple elastic-plastic laws (Weiner 1963, Grill, 1976, Wimmer, 1996). Later, separate creep laws were added (Rammerstrofer, 1979, Kristiansson, 1984). With the rapid advance of computer hardware, more computationally challenging elastic-viscoplastic models have been used (Zhu 1993, Boehmer 1998, Farup, 2000, Li, 2004, Risso, 2006, and Koric, 2006) which treat the phenomena of creep and plasticity together since only the combined effect is measurable. While Langrangian description of this process with fixed mesh is mostly adopted due to its easy implementation, an alternative mechanical model based on Eularian-Langrangian description has been proposed lately (Risso 2006). Similarly, the integration of viscoplastic laws ranges from easy-to-implement explicit methods (Morgan, 1978), to robust but complex implicitly based algorithms (Zhu, 1993, Li, 2004, Koric, 2006).
The work of Koric et al (Koric, 2006) implemented a robust local viscoplastic integration schemes from an in-house code CON2D (Zhu, 1993, Li 2004) into the commercial finite element package Abaqus/Standard via its user defined material subroutine UMAT (Dassault Systémes Simulia, 2012) including the special treatment of liquid/mushy zone. He later implemented an explicit finite-element formulation of this method (Koric, 2009) into Abaqus/Explict for the first time, and demonstrated its significant advantages in scale-up for large three dimensional problems on parallel computers. He has lately developed a new enhanced latent heat method (Koric, 2010, 2011) to link spatially and temporally super heat fluxes produced by turbulent fluid flow creating an effective approach towards accurate multiphysics modeling of commercial metal solidification processes with Abaqus/Standard.

2. Governing Equations

The conservation of mass, momentum, and energy (Dantzig, 2001) are satisfied in the molten metal, solidifying shell, and solid mold using three different models and three different computational domains. Mass conservation for a material with constant density can be expressed mathematically as:

$$\rho\left(\nabla\cdot\boldsymbol{v}\right)=0 \tag{1}$$

where ρ is the mass density and $\boldsymbol{v}$ is velocity. Momentum conservation is satisfied by solving a version of the following mechanical equilibrium equation without body forces in each model:

$$\rho\left[\frac{\partial\boldsymbol{v}}{\partial t}+\boldsymbol{v}\cdot\left(\nabla\boldsymbol{v}\right)\right]=\nabla\cdot\boldsymbol{\sigma} \tag{2}$$

where $\boldsymbol{\sigma}$ is the Cauchy stress tensor. Boundary conditions are either fixed displacement/velocity, or surface tractions applied in the form of normal pressure and tangential shear stresses. Each model also solves the following energy conservation equation, for a system without viscous dissipation and internal heat sources:

$$\rho\left[\frac{\partial H}{\partial t}+\boldsymbol{v}\cdot\nabla H\right]=\nabla\cdot\left(\boldsymbol{k}\cdot\nabla T\right) \tag{3}$$

where H is temperature-dependent specific enthalpy that includes the latent heat of solidification, T is temperature, $\boldsymbol{k}$ is the temperature-dependent thermal conductivity tensor, simplified in all domains to $\boldsymbol{k}\,\boldsymbol{I}$ by assuming isotropy. Boundary conditions are prescribed temperatures or heat flux, the latter often in the form of a convection condition.

3. Thermo-mechanical Constitutive Model of Solidifying Shell and Mold

The rate representation of total strain in this elastic-viscoplastic model is given by Equation 4:

$$\dot{\boldsymbol{\varepsilon}}=\dot{\boldsymbol{\varepsilon}}_{\text{el}}+\dot{\boldsymbol{\varepsilon}}_{\text{ie}}+\dot{\boldsymbol{\varepsilon}}_{\text{th}} \tag{4}$$

where $\dot{\boldsymbol{\varepsilon}}_{\text{el}},\dot{\boldsymbol{\varepsilon}}_{\text{ie}},\dot{\boldsymbol{\varepsilon}}_{\text{th}}$ are the elastic, inelastic, and thermal strain rate tensors respectively. Viscoplastic strain includes both strain-rate independent plasticity and time dependant creep. Creep is significant at the high temperatures of the solidification processes and is indistinguishable from plastic strain. Kozlowski (Kozlowski, 1992) proposed a unified formulation with the following functional form to define inelastic strain.

$$\dot{\bar{\varepsilon}}_{ie}[\text{sec}^{-1}]=f_C\left(\bar{\sigma}[\text{MPa}]-f_1\,\bar{\varepsilon}_{ie}\,|\,\bar{\varepsilon}_{ie}\,|^{f_2-1}\right)^{f_3}\exp\left(-\frac{Q}{T[K]}\right)$$

where:

$$Q=44,465$$

$$f_1=130.5-5.128\times10^{-3}T\,[\text{K}]$$

$$f_2=-0.6289+1.114\times10^{-3}T\,[\text{K}]$$

$$f_3=8.132-1.54\times10^{-3}T\,[\text{K}]$$

$$f_C=46,550+71,400\,(\%C)+12,000\,(\%C)^2 \tag{5}$$

Q is activation constant, and $\mathrm{f}_1,\mathrm{f}_2,\mathrm{f}_3,\mathrm{f}_{\mathrm{C}}$ are empirical temperature, and steel-grade-dependant constants. Another constitutive law, the modified power-constitutive model developed by Zhu (Zhu, 1993), is used to simulate the delta-ferrite phase, which exhibits significantly higher creep rates and lower strength than the austenite phase. The system of ordinary differential equations defined at each material point by the viscoplastic model equations is converted into two "integrated" scalar equations by the backward-Euler method and then solved using a special bounded Newton-Raphson method in user subroutine UMAT (Koric, 2006) linked with

Abaqus/Standard which solves the governing Equations 1 and 2.

Two-way thermo-mechanical coupling between the shell and mold is needed because the stress analysis depends on temperature via thermal strains and material properties, and the heat conducted between the mold and steel strand depends strongly on distance between the separated surfaces calculated from the mechanical solution. Heat transfer across the interfacial gap between the shell and the mold wall surfaces is defined with a resistor model that depends on the thickness of gap calculated by the stress model (Koric, 2006, 2009, 2011) and coded in GAPCON subroutine (Dassault Systémes Simulia, 2012) in Abaqus/Standard.

4. Fluid Flow Model in Liquid Pool

A 3-D fluid flow model of the liquid pool of molten steel solves for the time-averaged velocity and pressure distributions in an Eulerian domain. The fluid flow model is constructed for an incompressible Newtonian fluid, so Equation 1 simplifies to a divergence-free velocity field, and the constitutive relationship for the Cauchy stress tensor is:

$$\boldsymbol{\sigma} = C_{\mu} \frac{K^2}{\in} \left(\nabla \boldsymbol{v} + \left(\nabla \boldsymbol{v} \right)^T \right) - p\boldsymbol{I} \tag{6}$$

where p is pressure, constant C_{μ} is 0.09, and the turbulent kinetic energy K, and its dissipation $\in$, are found by solving two additional transport equations using the standard K-$\in$ model for turbulence. Buoyancy forces are negligible relative to the flow inertia, as indicated by $Gr/Re^2 \sim 10^{-2}$-10^{-4}, where Gr is the Grashoff number and Re is the Reynolds number. The governing equations are solved using the finite-volume method with the SIMPLE method and first-order upwind, as explained elsewhere (Versteeg, 2008) to give the pressure, velocity, and temperature fields and the heat flux at the domain boundary surfaces.

The shape of the domain is specified by extracting the position of the solidification front (liquidus temperature) from the solidifying shell model, and the symmetry planes of the mold. The effect of shell growth is incorporated as mass and momentum sinks (Rietow, 2007) in a user-defined function.

5. Fluid Shell Interface

Results from the fluid flow model of the liquid domain affect the solidifying shell model by the heat flux crossing the boundary, which represents the solidification front, or liquidus temperature. This "superheat flux" q_{super} can be incorporated into a fixed-grid simulation of heat transfer phenomena in the mushy and solid regions by enhancing the latent heat (Koric, 2010) in

Equation 1. This enables accurate uncoupling of complex heat-transfer phenomena into separate simulations of the fluid flow region and the mushy-solid region. Starting with the Stefan interface condition (Dantzig, 2001), the additional latent heat ΔH_f to account for superheat flux delivered from the liquid pool can be calculated from:

$$\Delta H_f = \frac{q_{super}\left(\boldsymbol{x},t\right)}{\rho_{solid}\left|v_{interface}\right|} \tag{7}$$

The latent heat enhancement is added to the original latent heat and enthalpy in Equation 3 via a UMATHT (Dassault Systémes Simulia, 2012) user subroutine (Koric, 2010, 2011) in Abaqus/Standard.

6. Multiphysics Model of Beam Blank Caster

The entire multiphysics model was applied to solve for fluid-flow, temperature, stress, and deformation in a complex-shaped beam blank caster under realistic continuous casting conditions. Fig. 1 shows a cross section of a typical beam blank caster. The generalized plane strain thermo-mechanical model in Abaqus/Standard of solidifaying shell traveling down the mold exploits the two-fold symmetry of the mold.

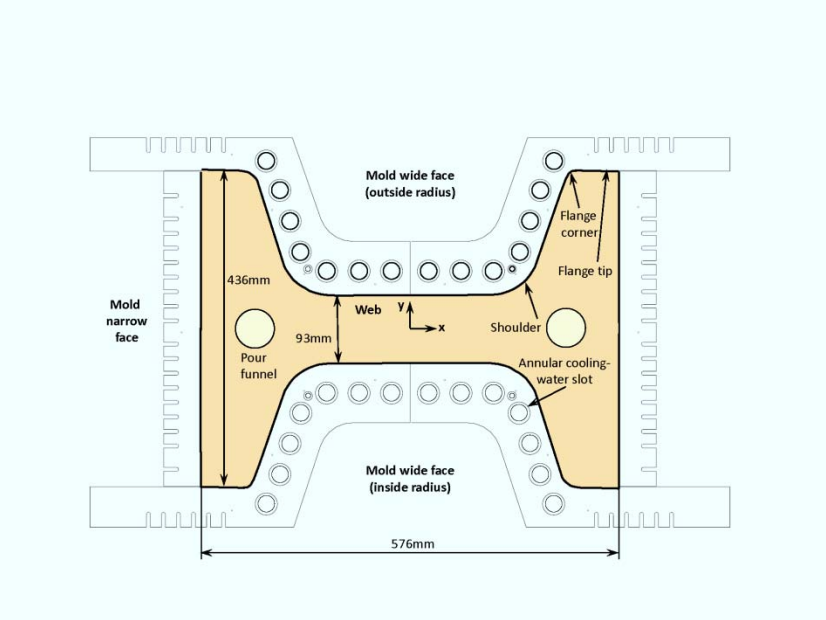

Figure 1. Schematic of beam blank caster (top view)

First, the thermo-mechanical model of the solidifying shell is run assuming a uniform superheat distribution driven by the temperature difference between T_{init} and T_{liq}, and artificially increasing thermal conductivity in the liquid region by 7-fold. The heat fluxes leaving the shell surface provide the boundary conditions for the thermo-mechanical model of the mold, which in turns supplies the next run of the shell model with mold temperature and thermal distortion boundary conditions. The position of the solidification front in the shell model defines an approximate shape of the liquid pool for the fluid flow model, which is used to calculate the superheat flux distribution. Finally, an improved thermo-mechanical model of solidifying shell is re-run which includes the effects of the superheat distribution and mold distortion, and completes the first iteration of the multiphysics model. Because the shell profile from the improved thermo-mechanical model has little effect on superheat results in the liquid pool, a single multiphysics iteration is sufficient to produce an accurate shell growth prediction.

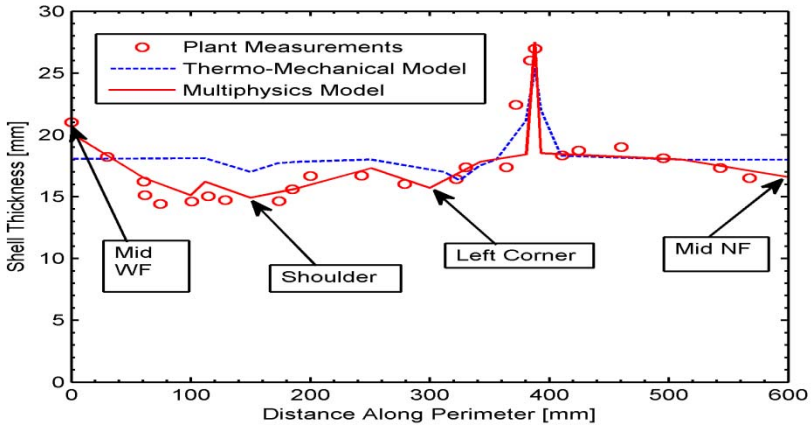

Figure 2. Shell Thickness Comparisons

The shell thickness at 90% liquid predicted by initial thermo-mechanical only and the full-multiphysics models is compared with measurements around the perimeter of a breakout shell obtained from a commercial caster (Hibbeler, 2009) in Fig. 2, while the maximum and minimum principal shell stress contours at 457 mm below the meniscus are given in Fig. 3.

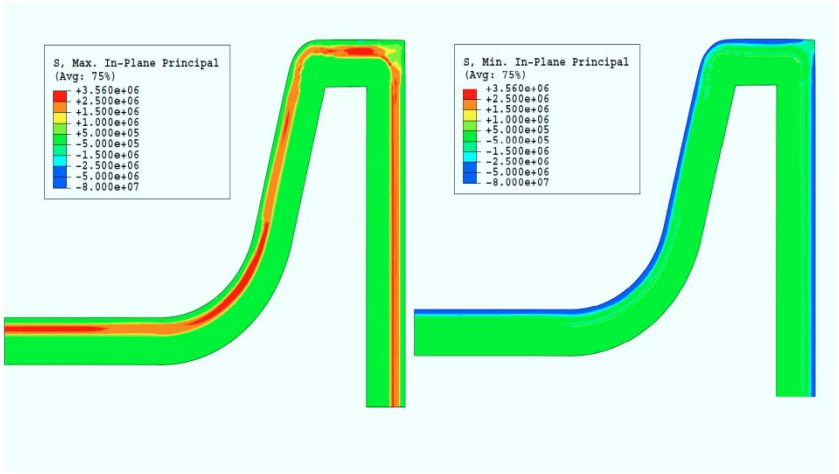

Figure 3. Max, and Min. principal stress contours 457 mm below meniscus

The initial thermo-mechanical model assuming a uniform superheat distribution can only roughly match the shell thickness variations. Shell thickness variations at the corners and shoulder due to air gap formations were captured owing to the interfacial heat transfer model.

However, the middle portion of the wide face is 4 mm thicker in the measurement. This is evidently caused by the uneven superheat distribution due to the flow pattern in the liquid pool, as this location is farthest away from the pouring funnels and has the least amount of superheat as shown in Fig 4.

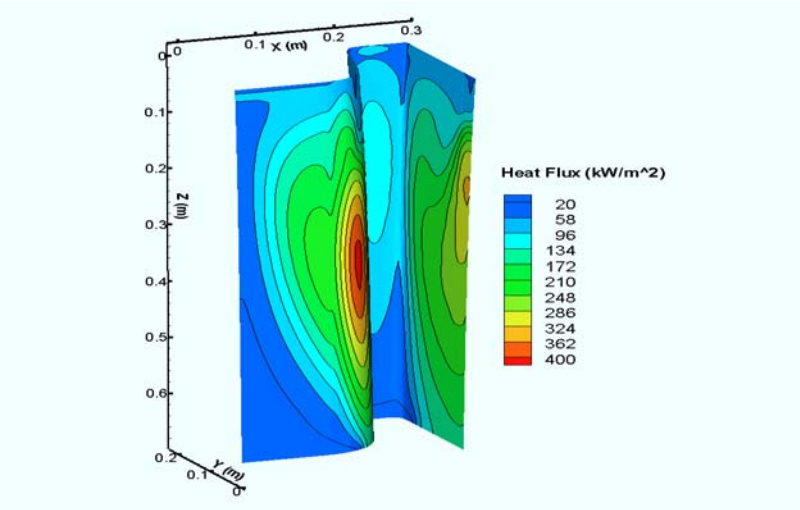

Figure 4. Superheat flux distribution

In contrast, the shoulder region receives the highest amount of superheat, so the measured shell thickness there is more than 2 mm thinner than the initial thermo-mechanical model prediction. The improved multiphysics model that includes the fluid flow effects matches the shell thickness measurement around the entire perimeter much more accurately.
The stress contours from Fig. 3 reveal expected compressive shell behavior at the "cold" surface and tensile stress in the hot interior near the solidification front. Maximum stress and strain is found in the shoulder area which is not a surprise since the thinner shell in this region caused by gap formation leads to stress concentration. Longitudinal cracks and breakouts are often found in this same shoulder region, as revealed by plant observations

7. Conclusions

The model developed in this work enables accurate modeling of complex multiphysics phenomena in continuous casting into separate simulations of the solidifying shell region, the fluid flow region, and the mold. Enahnced latent-heat method is applied to link spatially and temporally non-uniform super heat fluxes, produced by turbulent fluid flow and mixing in the liquid pool into a coupled thermo-mechanical model of continuous casting using a finite-element model in Abaqus/Standard using 4 different user defined subroutines The realistic effect of mold thermal distortion is incorporated through a second database and boundary condition at the shell-mold interface. The complete multiphysics model is applied to simulate solidification in a one-quarter transverse section of a commercial beam blank caster with complex geometry, temperature dependent material properties, and realistic operating conditions. The results compare well with in-plant measurements of the thickness of the solidifying shell. These findings illustrate the improved accuracy that is possible by including the effects of fluid flow into a thermal stress analysis of solidifying shell.

8. References

1. Abaqus Users Manual, Version 6.11-1, Dassault Systémes Simulia Corp., Providence, RI.
2. J.R. Boehmer, G. Funk, M. Jordan and F.N. Fett, "Strategies for coupled analysis of thermal strain history during continuous solidification processes,"Advances in Engineering Software, vol. 29 (7-9) pp. 679-697, 1998
3. J. A. Dantzig, C. L. Tucker III, "Modeling in Materials Processing, 1st ed.", pp. 282-321, Cambridge University Press, Cambridge, UK, 2001.

4. I. Farup and A. Mo,"Two-phase modeling of mushy zone parameters assosicated with hot tearing," Metall. Mater. Trans., vol. 31, pp. 1461-1472, 2000
5. A. Grill, J.K. Brimacombe, and F. Weinberg,"Mathematical analysis of stress in continuous casting of steel,"Ironmaking Steelmaking,vol 3, pp. 38-47, 1976
6. L. C. Hibbeler, S. Koric, K. Xu, C. Spangler, B. G. Thomas, "Thermomechanical Modeling of Beam Blank Casting", Iron and Steel Technology, vol. 6(7), pp. 60-73, 2009
7. S. Koric and B.G. Thomas, "Efficient Thermo-Mechanical Model for Solidification Processes,"International Journal for Num. Methods in Eng., vol. 66, pp. 1955-1989, 2006
8. S. Koric, L. C. Hibbeler, B. G. Thomas, "Explicit coupled thermo-mechanical finite element model of steel solidification", International Journal for Num. Methods in Eng., vol. 78, pp. 1-31, 2009
9. S. Koric, B. G. Thomas, V. R. Voller, "Enhanced Latent Heat Method to Incorporate Superheat Effects into Fixed-grid Multiphysics Simulations", Numerical Heat Transfer Part B, vol. 57, pp. 396-413, 2010
10. Koric S., L. C. Hibbeler, R. Liu, and B. G. Thomas, "Multiphysics Model of Metal Solidification on the Continuum Level," Numerical Heat Transfer B, 58, 371-392, 2011
11. P.F. Kozlowski, B.G. Thomas, J.A. Azzi, and H. Wang.,"Simple constitutive equations for steel at high temperature," Metallurgical Transactions, vol. 23A, pp. 903-918, 1992
12. J. O. Kristiansson," Thermomechanical behavior of the solidifying shell within continuous casting billet molds-a numerical approach,"Journal of Thermal Stresses, vol. 7, pp. 209-226, 1984
13. Chunsheng Li and B.G. Thomas, " Thermo-Mechanical Finite-Element Model of Shell Behaviour in Continuous Casting of Steel,"Metal and Material Trans. B, vol. 35B(6), pp. 1151-1172, 2004
14. K. Morgan , R. W. Lewis, and J. R. Williams ,"Thermal stress analysis of a novel continuous casting process," The Mathematics of Finite Elements and its Applications" Academic Press, vol. 3, 1978
15. F.G Rammerstrofer, C. Jaquemar, D.F. Fischer, and H. Wiesinger,"Temperature fields, solidification progress and stress development in the strand during a continuous casting process of steel," Numerical Methods in Thermal Problems, Pineridge Press, pp 712-722, 1979
16. B. Rietow, "Fluid Velocity Simulations and Measurements in Thin Slab Casting", MS Thesis, University of Illinois, 2007
17. J.M. Risso, A.E. Huespe, and A. Cardona,"Thermal stress evaluation in the steel continuous casting process," International Journal for Numerical Methods in Engineering, vol. 65(9), pp. 1355-1377, 2006
18. H. K. Versteeg, W. Malalasekera, "An Introduction to Computational Fluid Dynamics, Second Ed.", New York, NY:Pearson Prentice Hall, 2008
19. J.H. Weiner and B.A. Boley, "Elastic-plastic thermal stresses in a solidifying body," J. Mech. Phys. Solids, vol. 11, pp. 145-154, 1963
20. F. Wimmer, H. Thone, and B. Lindorfer,"Thermomechanically-coupled analysis of the steel solidification process in continuous casting mold, ", Abaqus Users Conference, 1996

21. H. Zhu," Coupled thermal-mechanical finite-element model with application to initial solidification.", Ph.D. Thesis, University of Illinois, 1993

Acknowledgement

The authors would like to thank the National Center for Supercomputing Applications (NCSA) at the University of Illinois for providing computing facilities.